



Correction of Real-Time Exposure in Hyperspectral Bands for Industrial Cameras

Yahya Dogan¹, Ahmet Cinar², Erdal Ozbay^{3*}

¹Computer Engineering Department & Siirt University, Turkey

^{2, 3*}Computer Engineering Department & Firat University, Turkey

¹ yahyadogan@siirt.edu.tr; ² acinar@firat.edu.tr; ^{3*} erdalozbay@firat.edu.tr

Abstract— *In this study, a new exposure correction method is presented for hyperspectral imaging. In the beginning, integration of the hardware parts to be used in the system is being done. Then a reference chart shows the minimum and maximum exposure values for each band is generated. Images with different exposure times have obtained in different hyperspectral bands using with an improved image acquisition interface. The various self-attributes that can represent the exposure situation have determined and a data set has created. The performance of Multilayer Sensor, Linear Regression and REPTree algorithms from artificial neural networks (ANN) models to determine the exposure quality is compared. The REPTree algorithm, which estimates the exposure situation 99.18%, is used for an application. It has been developed to determine the image with the highest exposure quality in the desired hyperspectral band and the results are discussed in this study.*

Keywords— *Exposure time, Exposure correction, Image processing, Artificial neural network, REPTree algorithm, Linear regression*

I. INTRODUCTION

In the cameras that have been developed at the present day, exposed images in the requested quality is not achievable in spite of their superior properties. A properly exposed image is dependent on many variables [1]. These are factors such as ISO value, aperture value and exposure time. ISO value can be defined as the light sensitivity of the optical sensors. Increase of the ISO value for one pause point doubles the light permeability, however, it is not preferred due to the fact that it causes noises in the image. Because of this, you need to work at low ISO values as long as possible. Aperture value controls how much density and intensity the rays reflected from objects will come to the receiver. Aperture value is expressed with f values (f1.0, f1.2, f1.4, f1.8, f2, f4, etc.). In each increase of the f value, the amount of light entering the machine decreases to the half of the previous one. Exposure time refers to the length of time for how long the light would fall on the media (film or optical sensor) on which the photo is taken. There are three situations with respect to whether or not the exposure time is arranged accurately. These are over, under and accurate or ideal exposure. Over exposure indicates the fact that the sensor is receiving more light than it should, and could result in the loss of details in the photograph, especially in the white brightness values. Under exposure indicates the situation in which the amount of light falling on the media is not enough, for this reason, the detail in the low pixel values are lost. Accurate or ideal exposure, however, indicates the fact that the amount of the light falling on the environment in which the photo is taken is at a desired level. In Fig. 1, different exposure situations that might occur have been shown.

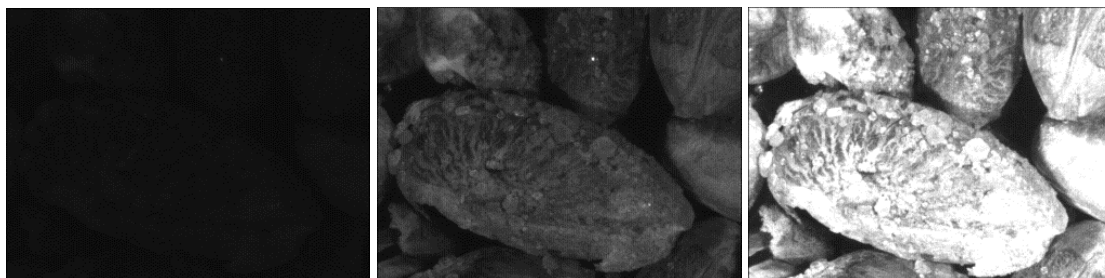


Fig. 1 (from left to right) Image that is obtained with under-exposure. Image that is obtained with ideal-exposure. Image that is obtained with over-exposure

Various studies have been made in the literature in order to correct the exposure situation in the photographs. In general, exposure can be examined in two groups as the exposure correction efforts, offline and real time. In offline exposure correction, the image is taken at first in the exposure period specified at the beginning, and the exposure of the current image is tried to be fixed with various methods. Here, the exposure period of the camera, re-access to the values such as ISO and aperture value is not at issue. Offline exposure correction is categorized in two groups such as manual and automatic. Many image correction tools (Adobe Photoshop, Google Picasa, Windows Live Photo Gallery, etc.) provide a way to correct the exposure manually. By using these types of tools, the users are allowed to change the pixel values and images of the histogram curve manually. In addition, the user can also operate on a region he or she wants. However, the manual exposure correction is a process which is both tedious and time consuming in terms of the user. Depending on the amount of images to be processed, the problem increases. On the other hand, it is possible to examine the automatic exposure correction in two parts as the global and local [2]. In Global Exposure Correction (GEC), a linear or non-linear function is used in order to match the tone values of an image with the desired values. The aforementioned function can be either predefined or obtained from a data set. Gamma correction and histogram equalization methods are frequently used in GEC [3, 4]. Another approach used in GEC, however, is Global Tone Mapping (GTM). By using different image decomposition methods in GTM (bilateral filter [5], trilateral filter [6], multi-scale Gaussians [7], discrete cosine transform [8] etc.) or luminance channels, the luminance layer of the image is made out. After that, the image contrast is drawn to a preferred range by using an appropriate global mapping technique [5-11]. In local exposure correction, the image is generally divided into pieces. In a study they made, Battiato et al. divided the image into N equal pieces. In the study in question, important cells are determined by using the contrast, histogram deviation and average values of each piece. The average pixel values of the remaining regions are brought to 128, and exposure is tried to be corrected [12]. In a study they made, Guo et al. determined the places where over exposure occurred by looking at the brightness and color values of the image. After that, they compressed the dynamic range of the regions with normal exposure values by using a tone mapping technique. Hence, due to the fact that the space of the regions where over exposure occurs, exposure is corrected to a certain extent [13].

Real-time exposure correction studies can also be examined in two sections as manual and automatic. In manual exposure correction, the user takes the first image and examine the histogram in terms of reference. As a result of the examination, he tries to find the image of the ideal exposure by optimizing the aperture value and exposure time parameters over the anomaly he detects on the histogram graphic [14]. In automatic exposure correction, the ISO values are generally set in the traditional cameras as a priority, and in the industrial cameras, however, the gain parameter is primarily set, and not too many changes are made on the value of the exposure time value. As it can also be understood from Fig. 2, this technical problem is created in hyperspectral imaging. The fact that the hyperspectral images taken by this method is of low-quality affects the performance of the analysis models developed in a bad way. In this study, the problem in question has been tried to be eradicated with a recommended machine learning-based approach.

In the second part of this statement, the problems encountered in hyperspectral imaging have been described in detail. In the third section, the hardware and software structure of the system that has been developed has been described. In the fourth section, however, the results that have been obtained have been scrutinized and the studies intended to be made in the future have been specified.

II. RELATED WORK

This work is most closely related with exposure time correction for hyperspectral imaging in the following two categories: Initially, we want to explain the problem definition and then description of system modulation.

2.1. Definition of the Problem

In hyperspectral imaging, from time to time undesirable situations (over exposure, under exposure) are encountered. In Fig. 2, hyperspectral images between 400 - 710 nm which have been taken in 10 nm each can be seen. While obtaining the images, all the parameters of the industrial camera were set to 'auto'. When, Fig. 2 is

carefully examined, it can be seen that 400 - 530, 560, 570 and 640 -710 under exposure has occurred in the images that have been taken in 400 - 530, 560, 570 and 640 - 710 bands. In the same way, when we look at the images obtained in 540, 550, 610 and 620 bands, bright areas have occurred because of over exposure. The overflows in the black and white luminescence (under and over exposure) have caused a lack of information in the images taken. In hyperspectral imaging, the best levels of conservation of information is required [15]. Fig. 2 indicates the fact that the standards used in the industrial cameras appear to be weak in the exposure quality of the images taken in the hyperspectral bands. For this reason, in the studies made, we see that generally the exposure times are manually set in the regional or band context [15]. In order to minimize information loss, a method that will automatically calculate the exposure times needs to be developed. In this study, we developed a software that operates at the base of a machine learning that can estimate an appropriate exposure time.

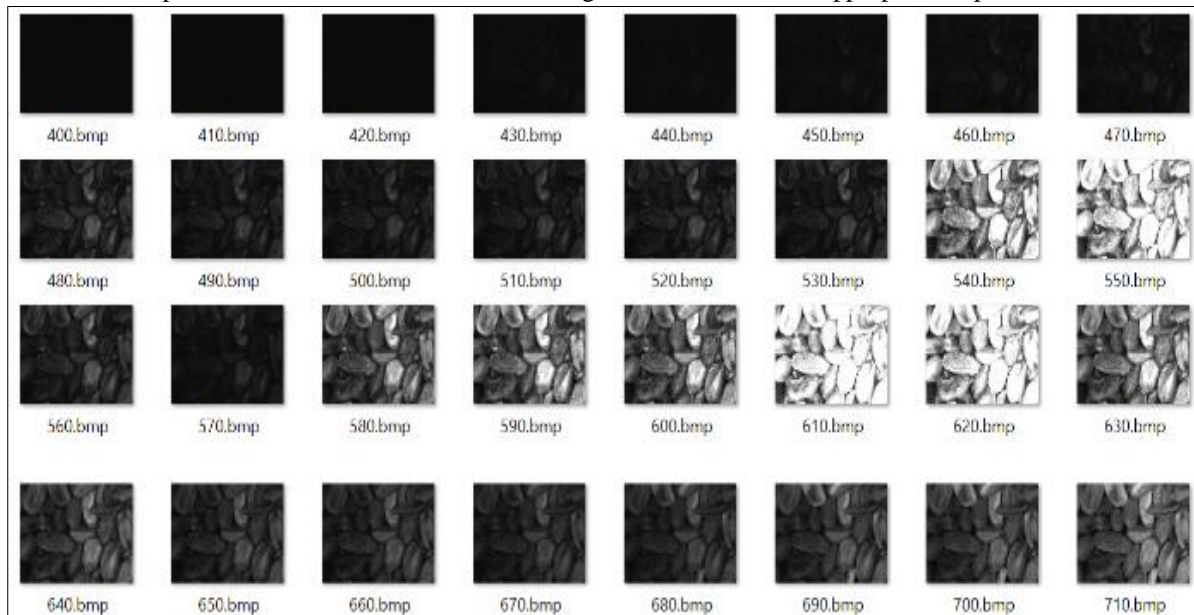


Fig. 2 The images obtained in different hyperspectral bands in the automatic mode of the industrial camera used in the study

2.2. Description of System Modulation

2.2.1 The Hardware Structure of the System

Hyperspectral Image System (HIS) consists of industrial camera (Imaging Source DMK 23G618), varispec adjustable filter and light sources (UV, halogen, xenon and led). In HIS, dark room has been designed for protection of images from the effects of the light sources in the external environment. In Fig. 3, the darkroom and HIS components can be seen.

Electronic adjustable filters are products which can be software-based controlled and adjustable to wavelength at the desired bandwidth (band pass filter) and which contains liquid crystal. In general, they are preferred in remote sensing and food safety works. Various models are available. In the study, Varispec VIS (visible spectrum) model has been used.

Wax paper has been put in front of the light source in order to prevent the rays from the light sources in in the dark room to hit the sample directly, and to create a homogeneous light distribution.



Fig. 3 Darkroom and HIS components

2.2.2 The Software Structure of the System

When an image will be taken at a particular spectral band image, the camera should be manually set to an appropriate exposure value and the related spectral band of the varispec filter. However, this process is difficult, time consuming and troublesome in terms of the user. In this study, a fast, consistent, reliable and user friendly software interface has been developed. With the application software that has been developed by using Java programming language and NetBeans 8.0.2 IDE, these problems have been tried to be solved. In Fig. 4, the interface of the software that we have developed can be seen.

In the software that has been developed, two "Interfaces" have been written in order to provide Access to the API's (dll) of the "Imaging Source industrial camera" and "Varispec electronic tunable filter". With the software developed by using JNA (Java Native Access), access to the devices is provided over these Interfaces.

In Fig. 4, the "set" button enables the exposure time of the camera used to the value given in the textbox. The "Property Dialog" button, however, provides access to properties of the camera. Here, camera parameters can be changed manually if desired. With the "connect to varispec" button, varispec access is provided over the port given in the textbox. And with the "disconnect" button, this connection is cut off. With "Get Varispec" button, varispec's band at that moment and the band range is enabled to be shown in the textboxes. "Set Varispec", however, positions the varispec filter to the values given in the textboxes.

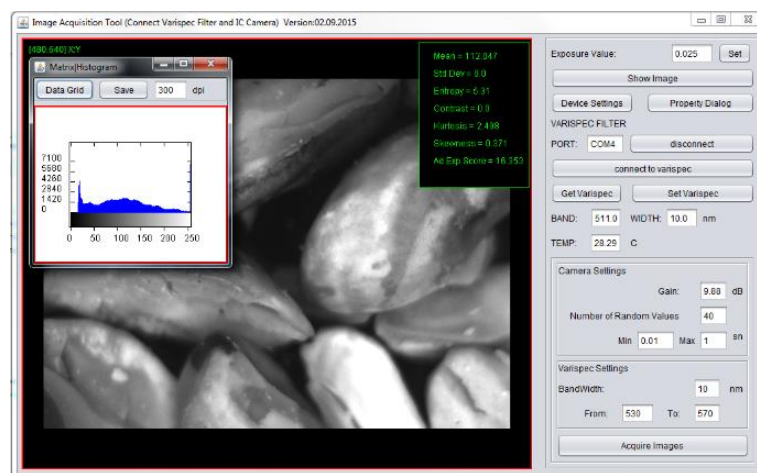


Fig. 4 The interface of the HIS application that has been developed

The process of taking a picture is enabled by clicking the "Build Image Dataset" button. Due to the fact that the change in the exposure time for each spectral band has an effect on a different proportion of the exposure status in an image taken, a reference chart containing the minimum and maximum exposure times shown in Table 1 has been prepared.

TABLE I
MINIMUM AND MAXIMUM EXPOSURE TIMES

Band	Min. Exposure Time (sec)	Max. Exposure Time (sec)
400, 410, 420	5	30
430	2	25
440	0,5	5,5
450	0,135	1,6
460	0,06	1,7
470	0,06	1,1
480	0,1	1,9
490	0,06	1,7
500	0,04	1,5
510	0,02	0,6
520	0,012	0,4
530	0,004	0,32
540, 550, 560	0,004	0,2
570, 580, 590	0,003	0,15
600, 610	0,003	0,16
620,630	0,003	0,18
640	0,005	0,2
650, 660	0,006	0,3
670	0,01	0,35
680, 690, 700, 710	0,011	0,35
720	0,02	0,5

When images are to be taken, a random of 30 images between the minimum and maximum exposure times for all spectral bands (33 pieces), and the data set has been created (990 pieces). After the data set has been created, the exposure quality of the images were wanted by two field specialists to be scored with real numbers in the range of 0 - 2, in a way that ‘0’ will show the lowest exposure, ‘1’ will show the correct exposure, and ‘2’ will show the most over exposure. These values constitute the output layer of the machine learning algorithms used.

A quality image is generally often the image is obtained by looking at its histogram. Attributes (mean, standard deviation, kurtosis, skewness and entropy) have been made out for the method recommended by using the interface in Fig. 5. These attributes that have been obtained constitute the input layer of ANN. The data set consists of 990 samples.

The depth sensor is able to send back images as if it was an ordinary camera, but instead of color, the pixel value represents the distance to the point. As such, the sensor can be seen as a range, or 3D camera. The basic technique of the depth sensor is to emit an infrared light with an IR laser diode, and calculate the depth from the reflection of the light at different positions using a traditional IR-sensitive camera.

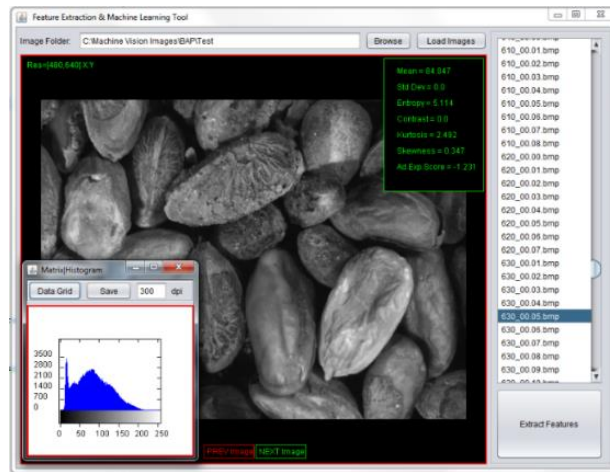


Fig. 5 Attribute extraction interface that have been developed

Arithmetic Mean

It is the value of the central location obtained by dividing the sum of the values of a main mass or a sample data by the number of terms in that main mass or sample size.

$$Aritmethic\ Mean = \frac{1}{N} \sum_{i=1}^N x_i \tag{1}$$

In Equation (1), N indicates the number of pixel, x_i indicates the gray color value of i . pixel.

Standard Deviation

It is a measurement used to summarize the spread of the data values. The standard deviation for a random variable or a probability distribution is expressed with σ . The standard deviation for the random variable X is calculated as follows:

$$Standard\ Deviation = \sqrt{\frac{1}{N} \left(\sum_{i=1}^N x_i^2 - \bar{x}^2 \right)} \tag{2}$$

In Equation (2) N indicates the total number of pixels, x_i indicates the gray color value of i . pixel, and \bar{x} indicates the gray color average in the pixels.

Skewness

It is the concept that expresses the data distribution getting away from the normal and taking the shape of a trapezoid that inclines to the right or to the left. In a normal distribution, the coefficient of skewness will be “zero”. As the skewness increases, the mode (the peak value of a symmetric distribution) and the average distance away from each other. The skewness coefficient may take values between – infinite and + infinite. Two

types of skewness may be referred to as positive and negative. If the average is smaller than the median, distribution will be skewed to the left (negative). If the average is larger than the median, the distribution will be skewed to the right (positive).

$$\text{Skewness} = \frac{\sqrt{N} \sum_{i=1}^N (x_i - \bar{x})^3}{(\sum_{i=1}^N ((x_i - \bar{x})^2))^{\frac{3}{2}}} \quad (3)$$

In Equation (3) N indicates the total number of pixels, x_i indicates the gray color value of the i . pixel, and \bar{x} indicates the grey color averaging in the pixels.

Kurtosis

It indicates how steep or flattened a normal distribution curve is. The kurtosis coefficient of a full bell curve is zero. If the kurtosis coefficient is positive, the curve is more steep compared to normal. If it is negative, it is more flattened compared to normal.

$$\text{Kurtosis} = \frac{N \sum_{i=1}^N (x_i - \bar{x})^4}{(\sum_{i=1}^N (x_i - \bar{x})^2)^2} - 3 \quad (4)$$

In Equation (4) N indicates the total number of pixels, x_i indicates the gray color value of the i . pixel, and \bar{x} indicates the grey color averaging in the pixels.

Entropy

Randomness of a system or a situation indicates uncertainty and the number or value of the probability of an unexpected situation to arise. According to Shannon, entropy is the expected value of the information carried by a transmitted message. The term called Shannon Entropy (H) is a value depending on the P_i probabilities belonging to all the a_i situations.

$$\text{Kurtosis} = \frac{N \sum_{i=1}^N (x_i - \bar{x})^4}{(\sum_{i=1}^N (x_i - \bar{x})^2)^2} - 3 \quad (5)$$

In Equation (5) N indicates the total number of pixels, x_i indicates the gray color value of the i . pixel, and P_{x_i} indicates the probability of x_i gray value.

Over the data set created by using the application in Fig. 5, REPTree, Multilayer Perceptron (MLP) and Linear Regression algorithms and 10 fold cross-validation test have been made, and the performance of the proposed method has been measured.

III. CONCLUSION

In this study, the performance of the system has been tested by using ANN's error propagation model or multilayer perceptron network model, which is also called backward propagation model, REPTree and Linear Regression algorithms. By using the algorithm which represents the problem most, the application correcting the real time exposure has been developed. Due to the fact that it is targeted to do all the work on a single platform, the application was carried out in the Java programming language. In the software that has been developed, open source code WEKA [16] and Open Cezeri Library (OCL) [17] have also been benefited from. For the parameters required in the study (iteration number, momentum coefficient, learning rate and activation function), values predefined in the WEKA program have been used.

In Fig. 6, 7 and 8, respectively, MLP several success criteria (R2, NSEC etc.) is indicated as the scatter diagram. In Fig. 6, 7 and 8, X axis specifies the observation values, and Y axis specifies the prediction values. In the conclusion of the test, for each algorithm, the correlation coefficient between the input variables used and the exposure status, the mean absolute error and model formation time have been shown in Table 2. When the table is examined, the values obtained point to how good the capacity of a generalization of the network is. It is seen that the correlation coefficient of the REPTree algorithm is higher compared to the other algorithms and that the mean absolute error is lower. The implementation of real time exposure correction developed as based on these values will take the REPTree algorithm as a basis.

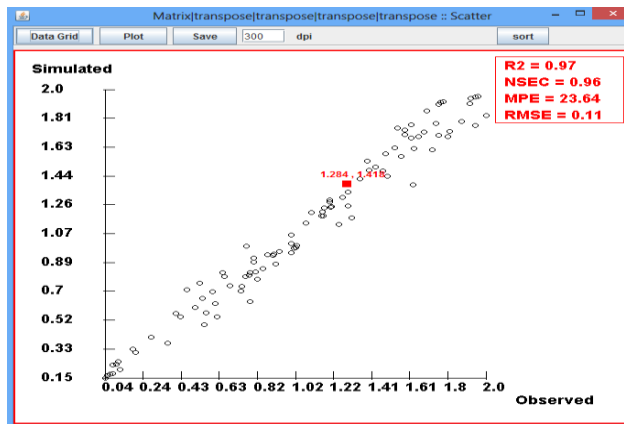


Fig. 6 MLP observation and prediction values scatter diagram

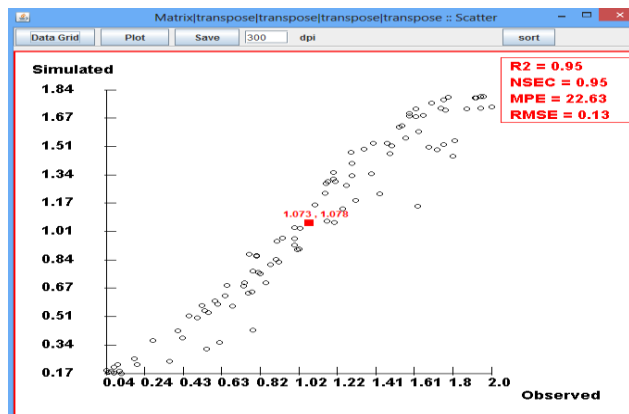


Fig. 7 Linear Regression observation and prediction values scatter diagram

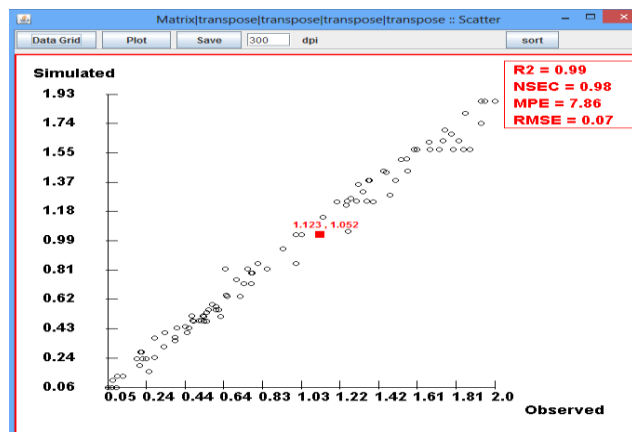


Fig. 8 REPTree observation and prediction values scatter diagram

TABLE III
THE CORRELATION COEFFICIENT OF THE CLASSIFIERS, THE MEAN ABSOLUTE ERROR AND MODEL FORMATION TIME

Classifiers	Correlation Coef. (%)	Mean Abs. Error (%)	Model Formation Time (sec)
Linear Regression	95.34	9.42	0.03
REPTree	99.18	6.18	0.03
MLP	97.12	7.96	0.36

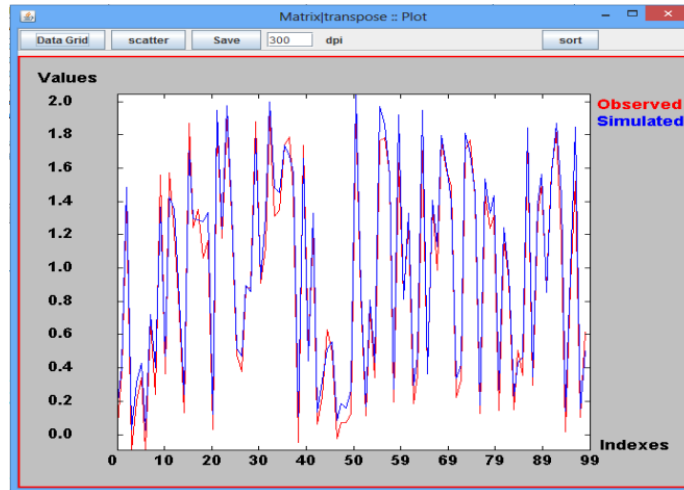


Fig. 9 MLP observation and prediction curves

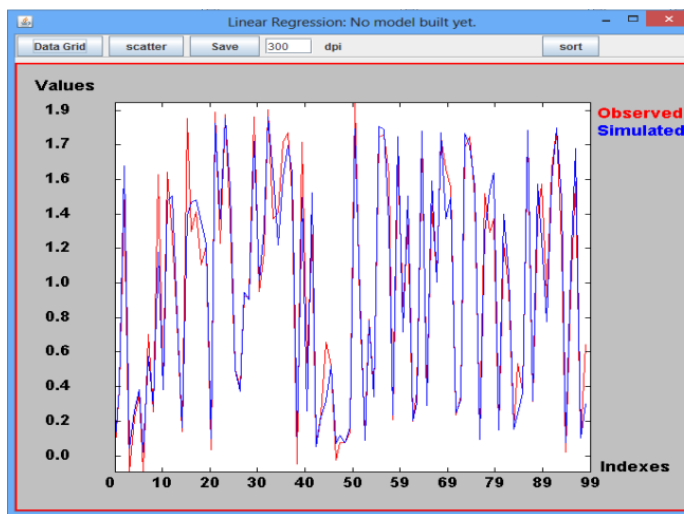


Fig. 10 Linear Regression observation and prediction curves

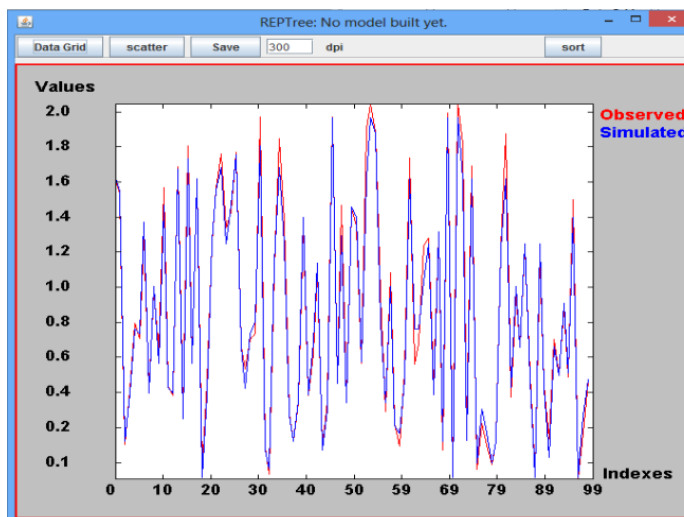


Fig. 11 REPTree observation and prediction curves

In Fig. 9, 10 and 11, however, observation and prediction curves obtained by using MLP, Linear Regression and REPTree Algorithms, respectively. In the graphics, X axis indicates the samples, and Y axis indicates the exposure values. When the graphics are examined, it is observed how successful the algorithms reviewed are in detecting the exposure status.

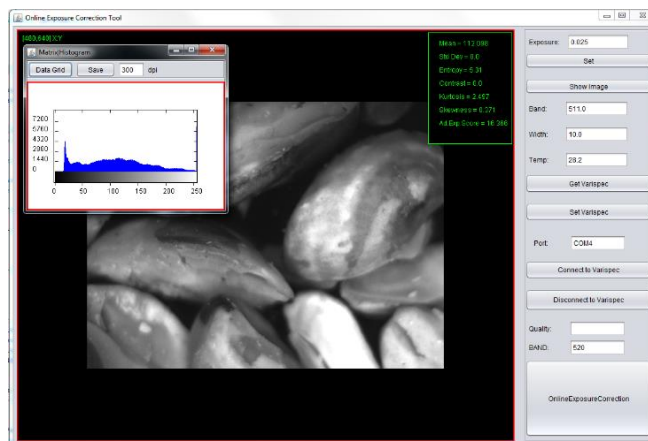


Fig. 12 Real time exposure correction interface

In Fig. 12, the interface of the application providing the exposure correction in the hyperspectral bands in real time has been shown. The system that has been developed tries to find the ideal exposure time with the loop mechanism within itself. In Fig. 12, the image with the most appropriate exposure time is determined for the band value entered when the “Online Exposure Correction” button is clicked, and it is recorded to the desired location. The loop mechanism that has been developed operates as follows.

- Set the number of steps (divide difference of the minimum and maximum exposure times of the related band to n pieces (n = 10))
- Set the Average Exposure Time (AET) for the related band
- Get images in the AET, AET -step, AET + step values
- Identify the quality of exposure based on REPTree algorithm
- If the exposure quality is the highest in OPS, save the image and terminate the application.
- Otherwise, repeat the steps below.
 - a) Meet the exposure qualities in AET - step and AET + step
 - b) Proceed in the direction in which the exposure quality is high
 - c) Increase the number of steps in each phase, and compare with the exposure quality of the previous image.
 - d) Save the last high quality image specified in the point in which the exposure quality starts to decline and terminate the application.

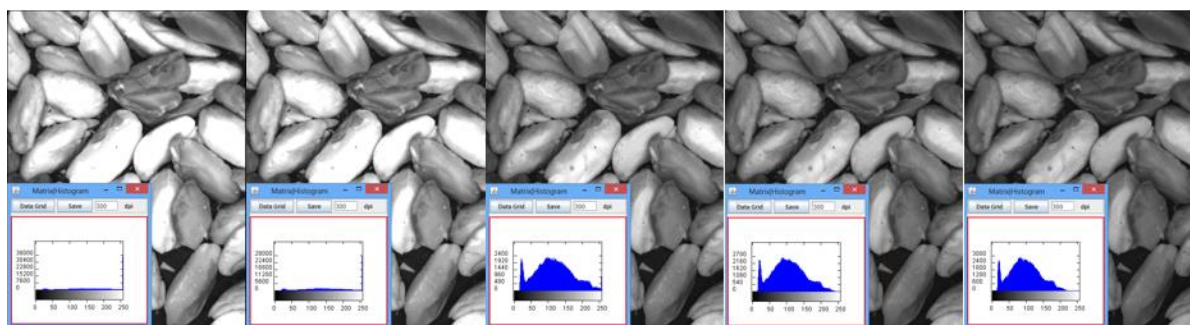


Fig. 13 The images produced by the program for the 600 nm band

In Fig. 13, the outputs of the real time exposure correction application that has been developed for the 600 nm band has been given. When the images were examined, over exposure occurred at beginning, and the exposure status was improved by reducing the exposure time. In Fig. 13, the last image is the output of the application.

In the continuation of study, it will be tried to find the attributes which have the most effect in detecting the status out of those used. The time cost will be reduced by using fewer attributes. In addition, the real-time mechanism that has been developed sometimes drops to local maximum. A loop mechanism will be developed in order to overcome this problem.

REFERENCES

[1] L. Kurnianggoro, V.D. Hoang, and K.H. Jo, “Calibration of a 2D laser scanner system and rotating platform using a point-plane constraint.” *Computer Science and Information Systems*, vol. 12, no. 1, pp. 307-322, 2015.

[2] Y. Wang, S. Zhuo, D. Tao, J. Bu, and N. Li, “Automatic local exposure correction using bright channel prior for under-exposed images.” *Signal Processing*, vol. 93, no. 11, pp. 3227-3238, 2013.

- [3] R.C. Gonzalez, and R.E. Woods, "Digital Image Processing." *Addison-Wesley Longman Publishing Co. Inc.*, Boston, USA. 2001.
- [4] S.M. Pizer, E.P. Amburn, J.D. Austin, R. Cromartie, A. Geselowitz, T. Greer, B.T.H. Romeny, and J.B. Zimmerman, "Adaptive histogram equalization and its variations." *Journal Computer Vision, Graphics and Image Process.*, vol. 39, no. 3, pp. 355-368, 1987.
- [5] F. Durand, and J. Dorsey, "Fast bilateral filtering for the display of high- dynamic-range images." *ACM Transactions on Graphics*, vol. 21, no. 3, pp. 257-266, 2002.
- [6] J. Shen, S. Fang, H. Zhao, X. Jin, and H. Sun, "Fast approximation of trilateral filter for tone mapping using a signal processing approach." *Signal Processing*, vol. 89, no. 5, pp. 901-907, 2009.
- [7] M. Ashikhmin, "A tone mapping algorithm for high contrast images." *in: Proceedings of Eurographics Workshop on Rendering, Eurographics Association*, pp. 145-156, 2002.
- [8] J. Mukherjee, and S.K. Mitra, "Enhancement of color images by scaling the DCT coefficients." *IEEE Transactions on Image Processing*, vol. 17, no. 10, pp. 1783-1794, 2008.
- [9] F. Drago, K. Myszkowski, T. Annen, and N. Chiba, "Adaptive logarithmic mapping for displaying high contrast scenes." *Computer Graphics Forum*, vol. 22, no 3, pp. 419-426, 2003.
- [10] T. Mertens, J. Kautz, and F.V. Reeth, "Exposure fusion: a simple and practical alternative to high dynamic range photography." *Computer Graphics Forum*, vol. 28, no. 1, pp. 161-171, 2009.
- [11] S. Battiato, A. Castorina, and M. Mancuso, "High-dynamic-range imaging for digital still camera." *International Society for Optics and Photonics*, pp. 324-335, 2002.
- [12] S. Battiato, A. Bosco, A. Castorina, and G. Messina, "Automatic image enhancement by content dependent exposure correction." *EURASIP Journal on Applied Signal Processing*, pp. 1849-1860, 2004.
- [13] D. Guo, Y. Cheng, S. Zhuo, and T. Sim, "Correcting over-exposure in photographs." *Computer Vision and Pattern Recognition*, pp. 515-521, 2010.
- [14] Exposure Factor Relationship Chart, [Online]. Available: <http://www.fredparker.com/ultexp1.htm#Light%20Intensity%20Chart> (current Sep 2017).
- [15] M. Ataş, Y. Yardimci, and A. Temizel, "A new approach to aflatoxin detection in chili pepper by machine vision." *Computers and Electronics in Agriculture*, vol. 87, pp. 129-141, 2012.
- [16] M. Hall, E. Frank, G. Holmes, B. Pfahringer, P. Reutemann, and I.H. Witten, "The WEKA data mining software: an update." *ACM SIGKDD Explorations Newsletter*, vol. 11, no. 1, pp. 10-18, 2009.
- [17] Open Cezeri Library, [Online]. Available: <https://github.com/hakmesyo/open-cezeri-library> (current Sep 2017).